XIX International Conference on Water Resources
CMWR 2012
University of Illinois at Urbana-Champaign
June 17-22, 2012

NUMERICAL MODELING OF NONLINEAR WATER WAVES WITH SIGMA COORDINATE AND LAYER THICKNESS OPTIMIZATION

Ling Zhu[*], Qin Chen[*] and Xiaoliang Wan[†]

[*] Louisiana State University
Department of Civil and Environmental Engineering, and Center for Computation and Technology
Baton Rouge, LA 70803 USA
e-mail: lzhu5@lsu.edu, qchen@lsu.edu

[†] Louisiana State University
Department of Mathematics, and Center for Computation and Technology
Baton Rouge, LA 70803 USA
e-mail: xlwan@math.lsu.edu

Key words: Euler equations, sigma coordinate, non-hydrostatic, layer thickness optimization

Summary. This paper presents a numerical model for simulating fully dispersive, nonlinear water waves in coastal areas. A finite difference method based on the Keller-Box scheme is used to solve the incompressible Euler equations with the free-surface boundary conditions. The sigma coordinate transformation maps the irregular physical domain with the wavy free surface and the uneven bottom to a rectangular computation domain. A pressure correction technique is utilized in this study, which splits the numerical procedure into hydrostatic and non-hydrostatic phases. An analytical dispersion relationship is derived from the discretized, linearized governing equations for layer thickness optimization. Numerical tests are presented to verify the model and compare with the analytical dispersion relationship.

1 INTRODUCTION

In physical oceanography, and coastal and ocean engineering, an accurate and efficient prediction of nonlinear surface waves is of paramount importance. Recent rapid advances in computational technology allow for solving Navier-Stokes equations (NSE) or Euler equations of motion directly to simulate free surface waves. For NSE based models[1, 2, 4, 5], the challenges are how to capture the nonlinear free surface motion, and how to preserve the dispersion properties due to the non-hydrostatic effect. To alleviate the difficulties for wave simulations in a large coastal area, the sigma coordinate has been introduced[3]. By mapping the physical domain with the free surface and the uneven bottom to a rectangular computational domain, the sigma coordinate transformation reduces the computational cost of tracking the free surface.

Typical NSE or Euler wave models need a sufficient number of vertical layers to achieve high dispersion accuracy. For deep water waves, the velocity and pressure are more uniform in the lower part of the water column but vary rapidly near the free surface, where a finer vertical resolution is required. Thus, better dispersion accuracy is expected for a non-uniform layer

arrangement in the deep water. However, caution needs to be taken to ensure that such a non-uniform layer arrangement does not introduce unacceptable dispersion errors in the intermediate water depth. This paper derives an analytical dispersion relationship from the discretized, linearized Euler equations, where the wave celerity is expressed as a function of the dimensionless wave number *kh* and layer thicknesses. By choosing proper layer thicknesses based on the derived dispersion relationship, we demonstrate that our model can cap the dispersion error below 1% for *kh* from zero to nine (or 2.88π) with only two vertical layers.

The paper is arranged as follows. In section 2, we describe the governing equations, boundary conditions, numerical algorithm, and model verification. We derive the analytical dispersion relationship of the model for two-layer thickness optimization in section 3, followed by a conclusion section.

2 MODEL DESCRIPTION AND VALIDATION

2.1 Governing equations and boundary conditions in sigma coordinate

For simulating the propagation of fully dispersive, nonlinear water waves, the governing equations are the continuity and momentum equations in the Cartesian coordinate (x^*, z^*) and time t^* without the viscosity and turbulence terms. We normalize the pressure p by the water density, and split it into hydrostatic and non-hydrostatic parts, as follows:

$$p = g(\eta - z^*) + q \tag{1}$$

where, g is the gravitational acceleration, η is the free surface elevation, and q represents the non-hydrostatic pressure. The vertical coordinate points upward with the origin sitting on the still water level.

The physical computational domain is vertically bounded by the bottom $z^* = -h(x^*)$ and the free surface $z^* = \eta(x^*, t^*)$. To deal with the uneven bottom and the time dependent free surface, the σ-coordinate is adopted in this study as follows:

$$t = t^*, \quad x = x^*, \quad \sigma = \frac{z^* + h}{D} \tag{2}$$

where $D = \eta + h$. The mapped computational domain is a stationary rectangular area, where σ ranges from 0 to 1 corresponding to the bottom and the free surface, respectively. Based on the chain rule, the governing equations in the σ-coordinate (x, σ, t) take the form

$$\frac{\partial u}{\partial x} + \frac{\partial u}{\partial \sigma}\frac{\partial \sigma}{\partial x^*} + \frac{\partial w}{\partial \sigma}\frac{\partial \sigma}{\partial z^*} = 0 \tag{3}$$

$$\frac{\partial u}{\partial t} + u\frac{\partial u}{\partial x} + w_\sigma \frac{\partial u}{\partial \sigma} + g\frac{\partial \eta}{\partial x} + \frac{\partial q}{\partial x} + \frac{\partial q}{\partial \sigma}\frac{\partial \sigma}{\partial x^*} = 0 \tag{4}$$

$$\frac{\partial w}{\partial t} + u\frac{\partial w}{\partial x} + w_\sigma \frac{\partial w}{\partial \sigma} + \frac{\partial q}{\partial \sigma}\frac{\partial \sigma}{\partial z^*} = 0 \tag{5}$$

where u and w are velocities in the x- and σ- direction, respectively, and

$$w_\sigma = \frac{D\sigma}{Dt^*} = \frac{\partial \sigma}{\partial t^*} + u\frac{\partial \sigma}{\partial x^*} + w\frac{\partial \sigma}{\partial z^*} \tag{6}$$

$$\frac{\partial \sigma}{\partial x^*} = \frac{1}{D}\frac{\partial h}{\partial x} - \frac{\sigma}{D}\frac{\partial D}{\partial x}, \quad \frac{\partial \sigma}{\partial z^*} = \frac{1}{D}, \quad \frac{\partial \sigma}{\partial t^*} = -\frac{\sigma}{D}\frac{\partial D}{\partial t} \tag{7}$$

The kinematic boundary conditions at the impermeable bottom and the free surface are

$$w\big|_{\sigma=0} = -u\frac{\partial h}{\partial x} \text{ and } w\big|_{\sigma=1} = \frac{\partial \eta}{\partial t} + u\frac{\partial h}{\partial x} \tag{8}$$

The depth-integrated continuity equation in the σ-coordinate now reads

$$\frac{\partial \eta}{\partial t} + \frac{\partial}{\partial x}\left[D\int_0^1 u d\sigma\right] = 0 \tag{9}$$

The continuity of normal stress at the free surface is enforced, which gives $q|_{\sigma=1} = 0$. At the inflow boundary, the velocity components and the surface elevation are specified by the linear wave theory; and at the outflow boundary, a sponge layer with a width of two wave lengths is employed to eliminate the wave reflection from the boundary.

2.2 Computational grid

The computational domain contains $NX \times NZ$ cells in x- and σ-directions, respectively. Denote the grids as

$$\left\{X \mid x_{i+1/2} = i\Delta x,\ i = 0,...,NX\right\} \text{ and } \left\{Z \mid \sigma_k = k\Delta\sigma,\ k = 0,...,NZ\right\} \tag{10}$$

The velocity components are distributed in a staggered way, where u and w are located at the four sides of cell (i+1/2, k+1/2) and (i, k), respectively. Following the reference[6], the pressure is placed at the same location as the vertical velocity on the layer interface. In this way the zero pressure condition at the free surface can be applied explicitly without interpolation. The free surface elevation, η, is also located at the cell face. Figure 1 illustrates the grid arrangements and distribution of all variables.

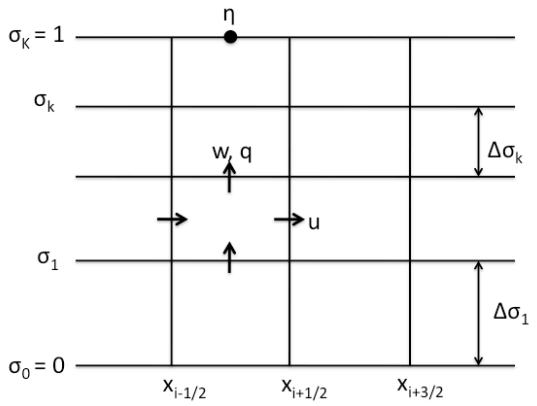

Figure 1: Schematic of grid and variable locations

2.3 Numerical procedure

A semi-implicit scheme[1] with a central difference in space is used to discretize the governing equations. The pressure correction technique is utilized in this study, which splits the numerical procedure into two phases to deal with the hydrostatic and non-hydrostatic parts of the pressure separately. In the hydrostatic phase, the horizontal momentum equation and the depth-integrated continuity equation are coupled as a closed system to solve for an intermediate horizontal velocity u^* and $\Delta\eta = \eta^{n+1} - \eta^n$. In the non-hydrostatic phase, the momentum equations and the continuity equation are coupled to solve for $\Delta q = q^{n+1} - q^n$. Then u and w will be updated.

The Poisson equation resulting from the pressure correction in the non-hydrostatic phase is solved with HYPRE, a library for solving large-scale linear systems of equations on massively parallel computers. The reader is referred to reference[6] for details of the numerical algorithm.

2.4 Model verification

Both standing wave and progressive wave tests are conducted. The numerical results are compared with the exact solution from the linear wave theory to verify the accuracy of this model. For the standing wave test case, a wave with an amplitude of 0.1 m is sloshing in a 20 m long closed basin with a water depth (h) of 20 m. The grid size is set to be Δx = 0.1 m and $\Delta\sigma$ = 0.5, respectively. The time step is set as $\Delta t = T/400$ s. The time series at x = 10 m is shown in the upper panel of Figure 2. For the progressive wave case, a wave train with an amplitude of 10^{-3} m and a wave length of 10 m is generated at the left end of a 160 m long flume with a water depth of 10 m. A 20 m long sponge layer is placed at the right end of the flume. The grid size is Δx = 0.2 m and $\Delta\sigma$ = 0.5, respectively. The time step is set as $\Delta t = T/800$ s. Notice that very high resolution is used for both horizontal and temporal discretization to eliminate truncation errors. Two vertical layers are used for both cases. The lower panel of Figure 2 shows the wave profile after 80 wave periods. We start the comparison with the analytical solution one wave length from the inflow boundary. Good agreement between the model and the exact solutions is found.

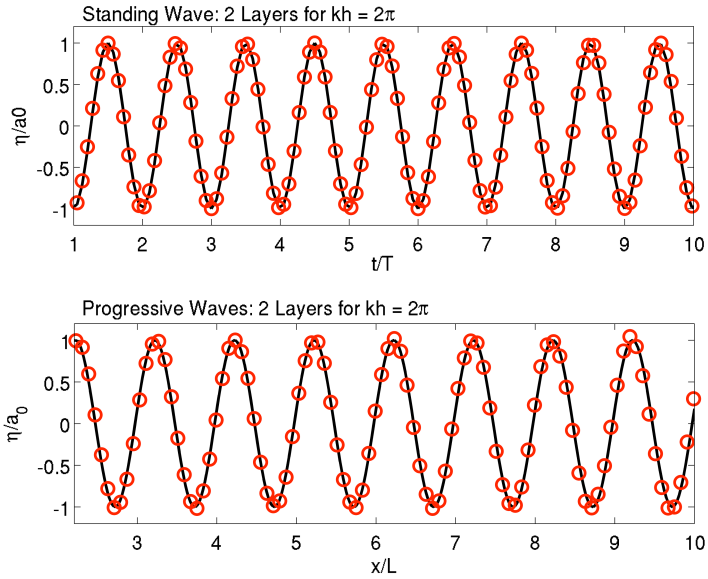

Figure 2: Comparison between numerical (circles) and exact (solid line) solutions for standing waves (top) and progressive waves (bottom) with 2 layers for kh = 2π

3 DISPERSION ANALYSIS

3.1 Linearized governing equations

The linearized governing equations in the Cartesian coordinate can be written as follows:

$$\frac{\partial u}{\partial x}+\frac{\partial w}{\partial z}=0 \tag{11}$$

$$\frac{\partial u}{\partial t}+g\frac{\partial \eta}{\partial x}+\frac{\partial q}{\partial x}=0 \tag{12}$$

$$\frac{\partial w}{\partial t}+\frac{\partial q}{\partial z}=0 \tag{13}$$

$$\frac{\partial \eta}{\partial t}+\frac{\partial}{\partial x}\int_{-h}^{\eta} u dz=0 \tag{14}$$

In this study, we only consider the 2-layer optimization while the procedure can be generalized straightforwardly to deal with a 3-layer case. Denote layer thickness as $(\Delta z_1, \Delta z_2) = (\alpha_1 h, \alpha_2 h)$, where Δz_k is the thickness of layer k, h is the water depth, α_k is the ratio of thickness of layer k to the water depth. By only considering the discretization in the vertical direction, we obtain the following semi-discrete vertical momentum equation:

$$\frac{1}{2}\left(\frac{\partial w_{k+1}}{\partial t}+\frac{\partial w_k}{\partial t}\right)+\frac{q_{k+1}-q_k}{\Delta z_{k+1}}=0,\ k=0,...,K \tag{15}$$

The Keller-box scheme is utilized and the vertical momentum equation is actually solved in the middle of the layer. A flat bottom is considered here. By substituting the bottom kinematic condition and the free surface condition, $q_2 = 0$, into Equation (15), the following equations are obtained:

$$\frac{\partial w_1}{\partial t}=-2\frac{q_1-q_0}{\alpha_1 h} \tag{16}$$

$$\frac{\partial w_2}{\partial t}=2\frac{q_1-q_0}{\alpha_1 h}+2\frac{q_1}{\alpha_2 h} \tag{17}$$

By taking the temporal derivative of Equation (11) and the spatial derivative of Equations (12), (16) and (17), and combining them together, we get

$$-g\frac{\partial^2\eta}{\partial x^2}-\frac{1}{2}\left(\frac{\partial^2 q_1}{\partial x^2}+\frac{\partial^2 q_0}{\partial x^2}\right)-2\frac{q_1-q_0}{\alpha_1^2 h^2}=0 \tag{18}$$

$$-g\frac{\partial^2\eta}{\partial x^2}-\frac{1}{2}\frac{\partial^2 q_1}{\partial x^2}+\frac{1}{\alpha_2 h}\left[4\frac{q_1-q_0}{\alpha_1 h}+2\frac{q_1}{\alpha_2 h}\right]=0 \tag{19}$$

Assume the pressure, the horizontal velocity and the surface elevation take the following forms $q_j = Q_j e^{i(kx-\omega t)}$, $u_j = U_j e^{i(kx-\omega t)}$, $\eta = A e^{i(kx-\omega t)}$, respectively. Substituting them into Equations (18) - (19) leads to a system of linear equations in terms of Q_0 and Q_1. After solving this system of equations, we get $Q_j = m_j \cdot gA$ with m_j expressed as

$$m_0=\frac{-2(a_1-a_2+a_3)(kh)^2}{(kh)^4+(a_1-2a_2+a_3)(kh)^2+a_1a_3} \tag{20}$$

$$m_1=\frac{-2(kh)^4-2(a_1-a_2)(kh)^2}{(kh)^4+(a_1-2a_2+a_3)(kh)^2+a_1a_3} \tag{21}$$

where $a_1 = 4/\alpha_1^2$, $a_2 = -8/\alpha_1\alpha_2$, $a_3 = 4/\alpha_2^2$.

By substituting q_0 and q_1 into Equations (12) and (14), a system of linear equations in terms of U_j and A is obtained:

$$\begin{bmatrix} -\omega & \alpha_1 kh & \alpha_2 kh \\ \left[1+\frac{1}{2}(m_0+m_1)\right]gk & -\omega & 0 \\ \left(1+\frac{1}{2}m_1\right)gk & 0 & -\omega \end{bmatrix} \begin{bmatrix} A \\ U_0 \\ U_1 \end{bmatrix} = \begin{bmatrix} 0 \\ 0 \\ 0 \end{bmatrix} \tag{22}$$

In order to get a non-trivial solution for U_j and A, the determinant of the matrix must be equal to zero, which leads to the following dispersion relation

$$\frac{\omega^2}{k^2} = gh\left\{\left[1+\frac{1}{2}(m_0+m_1)\right]\alpha_1 + (1+\frac{1}{2}m_1)\alpha_2\right\} \tag{23}$$

3.2 Verification and optimization

The derived dispersion relation is compared with the numerical results from the model. The progressive wave test case is used. The wave amplitude is set to be 10^{-4} m to avoid the effect of nonlinearity. Six test cases with kh of 0.25π, 0.5π, π, 1.5π, 2π and 2.5π are simulated and dispersion errors are quantified in comparison with the exact linear wave theory.

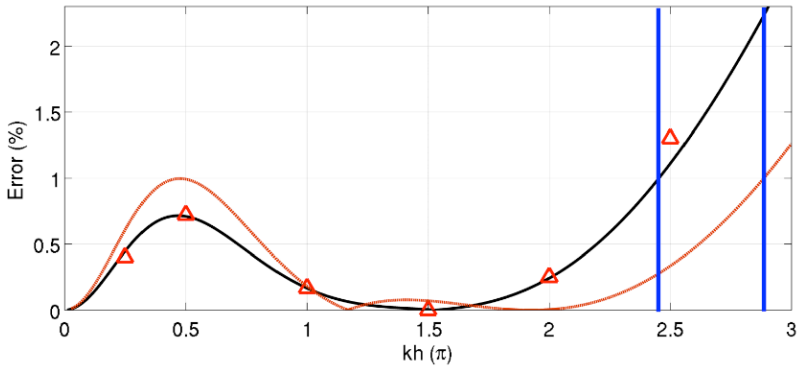

Figure 3: Comparison of numerical and analytical phase errors normalized by exact wave celerity. Triangles: numerical result with two equidistant layers; Black line: analytical result with two equidistant layers; Red dash line: analytical result with two optimized layers

Figure 3 shows that the dispersion errors of the numerical model are in good agreement with those predicted by the derived analytical dispersion relationship for the model with two uniform layers. Y-axis is the relative phase error normalized by the exact wave celerity of the linear wave theory. The red dash line in Figure 3 shows that by decreasing the top layer thickness to 33% of the water depth, the model can simulate waves with kh up to 2.88π with a phase error less than 1%. By contrast, it can only reach 2.4π theoretically with two equidistant layers.

5 CONCLUSIONS

- The paper presents a numerical model for simulating the propagation of fully dispersive, nonlinear water waves in coastal areas. The finite difference method based on the Keller-Box scheme and the pressure correction technique[7] is used to solve the Euler equations of motion in a sigma coordinate. Numerical results have demonstrated that the model with 2 equidistant layers is capable of simulating standing waves and progressive waves for $kh = 2\pi$ with a linear dispersion error less than 0.25% in comparison with the exact solution.
- An analytical dispersion relationship for the numerical model with two vertical layers has been derived by neglecting the temporal and horizontal discretization errors. The numerical phase error is in agreement with the prediction of the derived dispersion relationship, which provides us with a tool to optimize the layer thickness for the best model performance. It has been found that the two-layer model is able to simulate surface waves with a phase error less than 1% for a wide range of *kh* from 0 to 9 if the top layer is 33% of the water depth and the bottom layer is 67%.

ACKNOWLEDGEMENTS

The study was supported by the National Science Foundation (NSF) (CBET-0652859). Any opinions, findings and conclusions or recommendations expressed in this paper are those of the authors and do not necessarily reflect the views of the NSF.

REFERENCES

[1] V. Casulli, "A semi-implicit finite difference method for non-hydrostatic, free-surface flows", *Int. J. Numer. Meth. Fluids*, **30**, 425-440 (1999).
[2] M. B. Kocyigit, R. A. Falconer and B. Lin, "Three-dimensional numerical modeling of free surface flows with non-hydrostatic pressure", *Int. J. Numer. Meth. Fluids*, **40**, 1145-1162 (2002).
[3] P. Lin and C. W. Li, "A sigma-coordinate three-dimensional numerical model for surface wave propagation", *Int. J. Numer. Meth. Fluids*, **38**, 1045-1068 (2002).
[4] R. A. Walters, "A semi-implicit finite element model for non-hydrostatic (dispersive) surface waves", *Int. J. Numer. Meth. Fluids*, **49**, 721-737 (2005).
[5] H. Yuan and C. H. Wu, "Fully non-hydrostatic modeling of surface waves", *J. Eng. Mech.*, **132**, 447-456 (2006).
[6] M. Zijlema and G. Stelling, "Further experiences with computing non-hydrostatic free-surface flows involving water waves", *Int. J. Numer. Meth. Fluids*, **48**, 169-197 (2005).